

# Lecture 21

## Distribution of the Molecular Gas

1. Global Distribution of Gas
2. Atomic Hydrogen and GMCs
3. Formation
4. Internal Structure
5. Observing Molecular Cloud Cores

### References

Origins of Stars & Planetary Systems

<http://www.cfa.harvard.edu/events/1999crete>

Myers, “Physical Conditions in Molecular Clouds”

Blitz & Williams, “Molecular Clouds”

Lada, “The Formation of Low-Mass Stars”

# 1. Global Distribution of Molecular Gas

- Observing from inside makes it difficult to sort out the distribution of molecular gas in the Milky Way.
- The CO emission is inhomogeneous (radially and azimuthally).
- Confusion and kinematic ambiguity make it difficult to determine whether GMCs are primarily located in spiral arms.
- The X-factor is used to obtain the  $\text{H}_2$  surface density.
- $\text{H}_2$  has a ring (“5-kpc ring”) with a hole at the center (next slide).
- Higher angular resolution and observations of external galaxies are particularly useful.
- The total  $\text{H}_2$  and HI masses are of the same order, but the ratio is highly variable

# HI and H2 Column Densities

Hunter et al. ApJ 2001

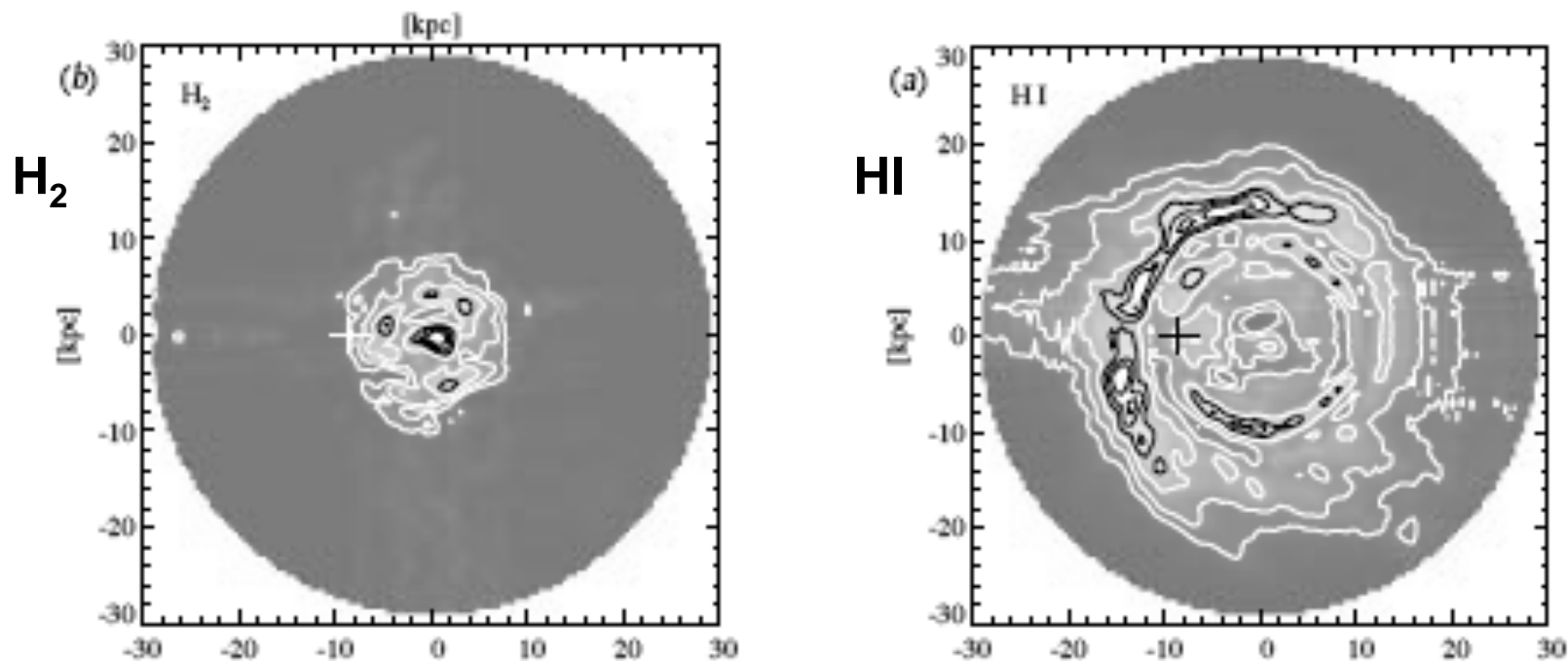
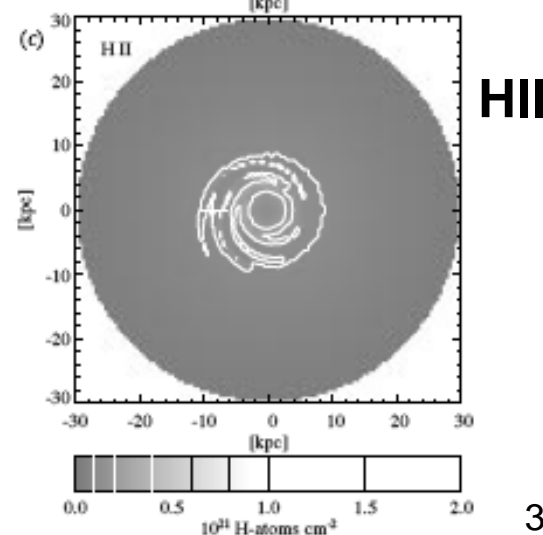


FIG. 8.—Total surface densities of (a) H I, (b) H<sub>2</sub>, and (c) H II as a function of position in the Galactic plane. The H I and H<sub>2</sub> plots have been smoothed to 2 kpc resolution. The position of the Sun is indicated with a cross. The gas densities are assumed to be zero beyond the 30 kpc Galactic radius limit of the calculation (see § 5).

- Modeling of  $\gamma$ -rays and CfA CO survey
- H<sub>2</sub> has a ring with a hole at the center
- Spiral arms are not delineated clearly



# FCRAO Outer Galaxy Survey

Heyer et al. ApJS 115 241 1998



- **Regions of little molecular gas**, perhaps cleared by photodissociation, stellar winds and supernova from massive stars. The last two processes can sweep up and compress gas and help make new stars.
- **CO is primarily in spiral arms**, with estimated  $H_2$  *arm-interarm* contrast  $\sim 30:1$  (the HI ratio is 2.5:1).
- **Popular old idea**: GMCs form by the compression of atomic gas as it crosses the spiral arms on the time scale of  $\sim 10^8$  yr.
- **Pervasive low-level CO** called “chaff” may account for 10% of the total molecular gas, estimated to be  $10^9 M_\odot$ , but it may not be enough to make GMCs.

# CO Emission from Spiral Arms

Heyer et al. ApJS 115 241 1998

The velocity-position diagram (bottom) separates the local and nearby Perseus arms and shows that the CO emission is localized in the arms.

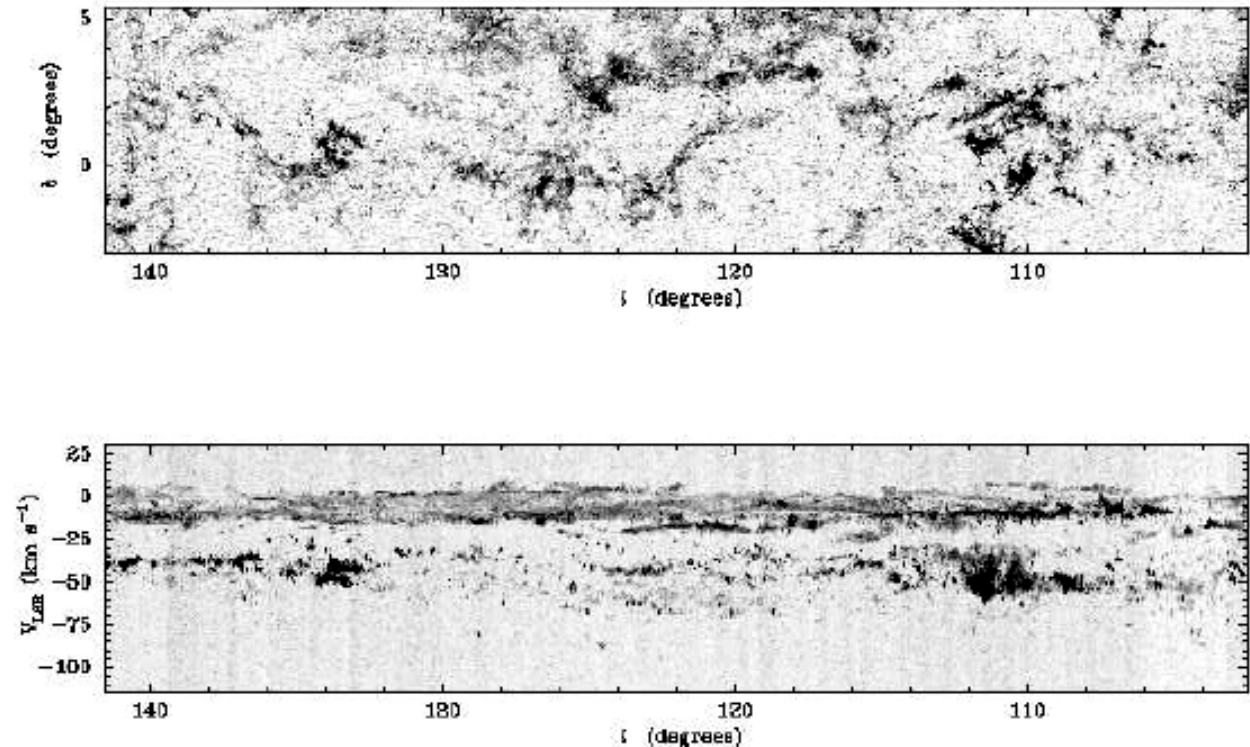
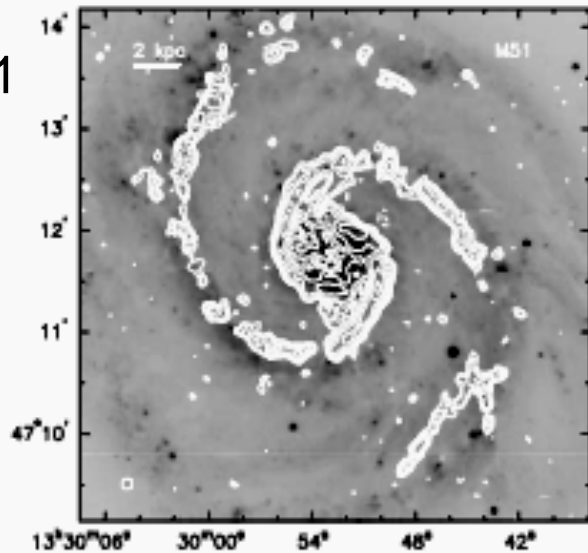


*Figure 2.* CO emission in the outer Galaxy (from Heyer et al. 1998). Top panel is a velocity integrated  $l-b$  plot, lower panel is a  $l-v$  plot (integrated over the latitude range of the survey) showing the local and Perseus spiral arms. Note the almost complete absence of molecular gas between the two spiral arms at about  $0 - -10 \text{ km s}^{-1}$  and  $-40 \text{ km s}^{-1}$ . The high spatial dynamic range of this survey shows the large scale distribution of molecular gas in the ISM in exceptional detail.

# GMCs and Spiral Arms

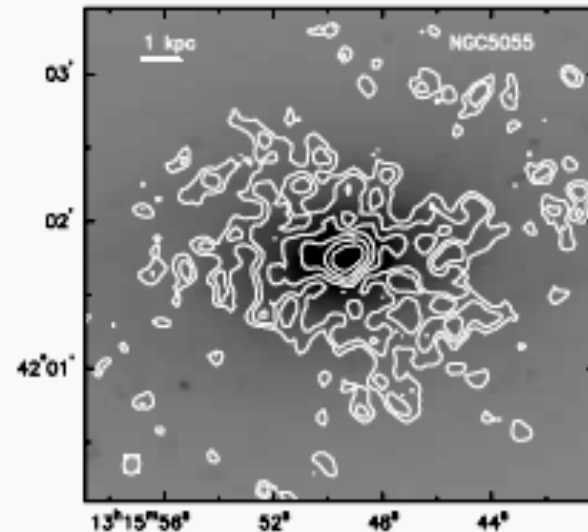
Blitz and Williams (1999)

M 51



classic grand spiral

NGC 5055



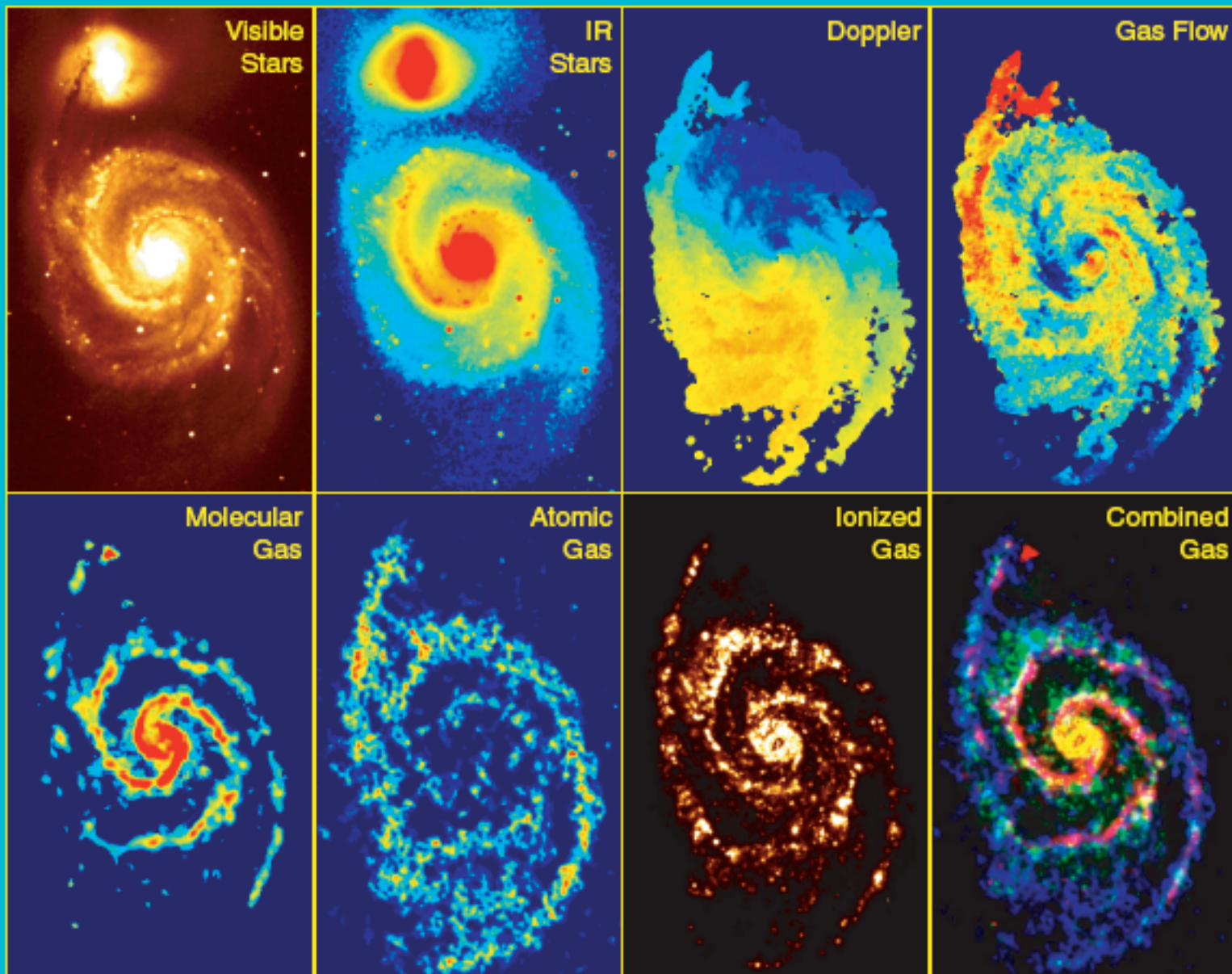
weak spiral structure

CO emission overlaid on optical photos

**Similar kinds of GMCS in galaxies with and without well-defined spiral structure. How do GMCs form in galaxies like NGC 5055 ?**

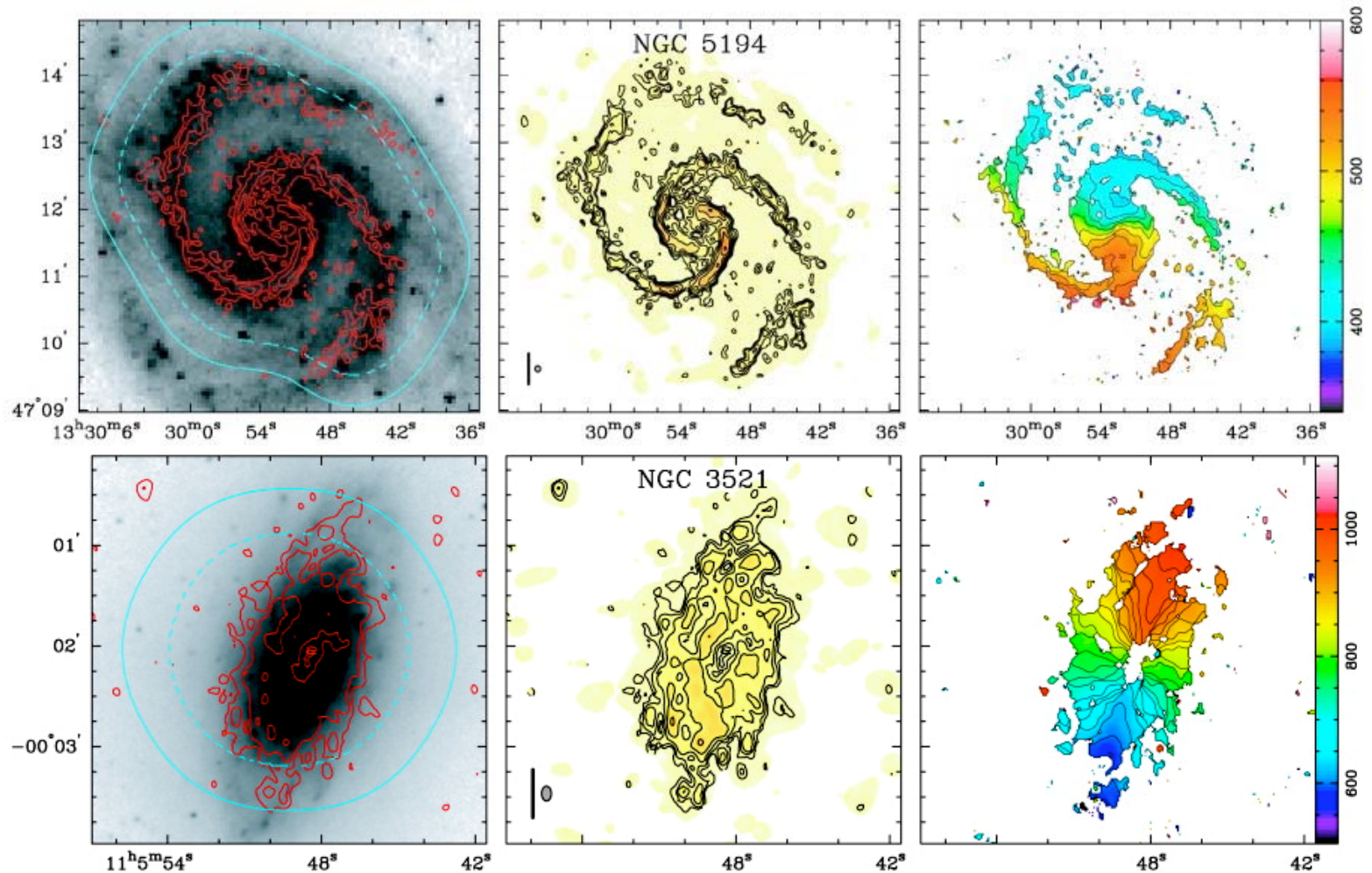


## The Spiral Arms of the Whirlpool Galaxy



# 6'' BIMA CO Survey Of Nearby Galaxies

Helfer et al. 2003 ApJS 145 259



CO emission overlaid on SDSS

CO emission

CO velocity



## 2. HI Content of GMCs

- HI envelopes around molecular clouds are common.
- Local GMCs have comparable masses of HI and H<sub>2</sub>
- HI is more spatially extended, e.g., 100-200 pc
- Origin of the HI in and near GMCs:
  - Photodissociation of H<sub>2</sub>?
  - Remains of the GMC formation from HI?
- HI properties of GMCs vary throughout the Milky Way, e.g., HI merges into a continuous background in the 5-kpc ring.

# HI and $^{13}\text{CO}$ in the Rosette Molecular Cloud

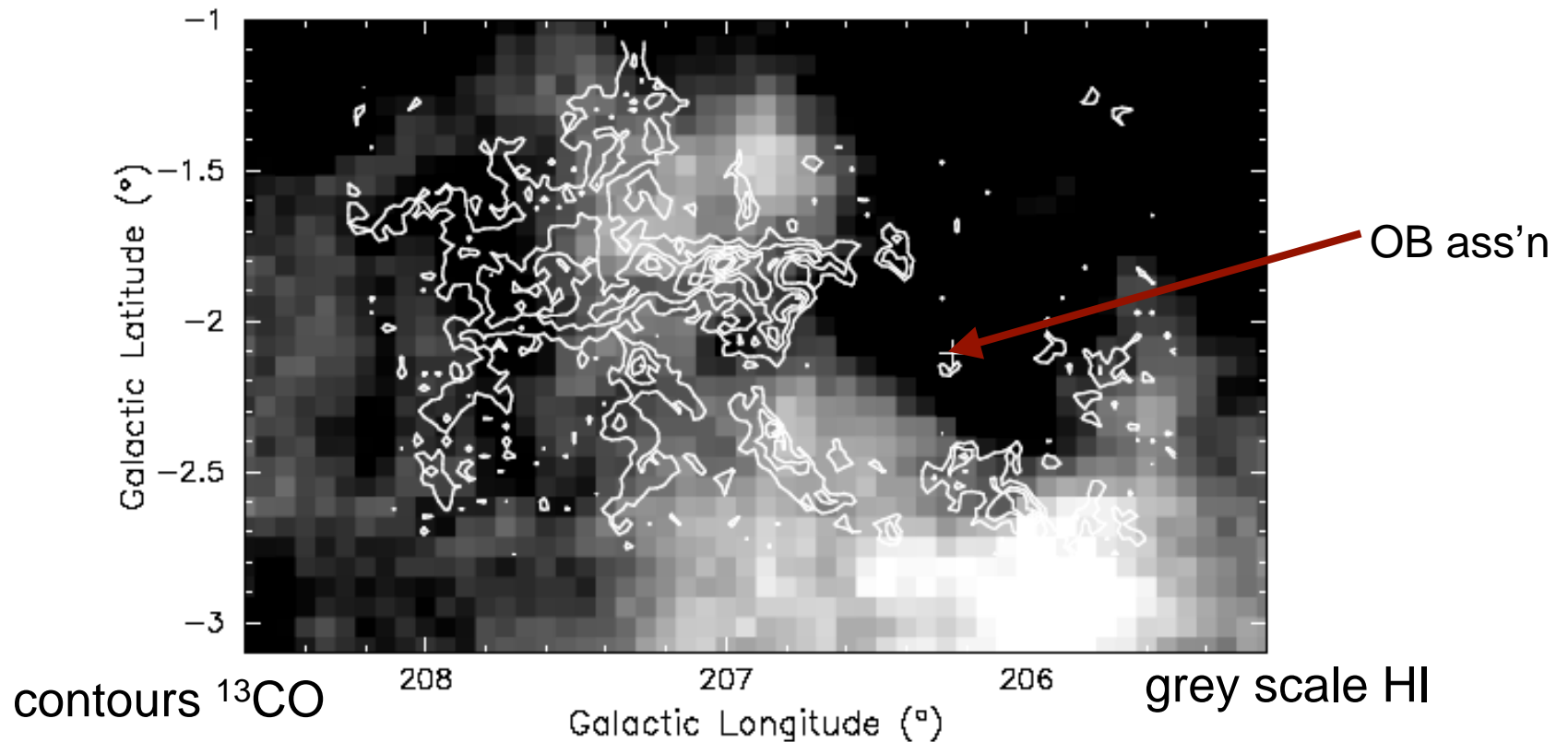


*Figure 3.* An HI envelope around the Rosette molecular cloud. The grayscale, range 450 to 620  $\text{K km s}^{-1}$ , shows HI data from Arecibo observations by Kuchar & Bania (1993). Contours, beginning from and with increment 18  $\text{K km s}^{-1}$ , are CO emission from Bell Labs observations by Blitz & Stark (1986). Emission has been summed over a velocity range  $v = 4 - 25 \text{ km s}^{-1}$ . The cross marks the OB association that lies at the center of the Rosette nebula and has cleared out the neutral gas. The regions of strong HI emission (lighter colors) lie on the CO cloud boundaries, forming an envelope around the cloud.

Blitz & Williams 1999

### 3. Formation of Molecular Clouds

#### *An Unsolved Problem*

Many processes are involved – gravity, magnetic fields, turbulence, shocks, radiation, etc., but which is dominant?

- Gravity must play a role since GMCs are self-gravitating, but low-mass clouds ( $M < 10^3 M_{\odot}$ ) are probably not, e.g., high-latitude clouds and the “chaff”.
- GMCs may be short lived, as indicated by the age of the oldest sub-associations (10-20 Myr) that are still associated with GMCs.
- In principle, the age should be greater than the crossing time, but the sound speeds are low. If the large observed line widths reflect MHD turbulence, we can interpret the measured dispersion as the Alfven speed. Applying the line width size relation leads to

$$R/\sigma \sim 2 \text{ Myr } (\sigma / \text{km s}^{-1}),$$

somewhat shorter than the above estimates of the lifetime of a GMC.

# Formation Mechanisms

Three ways are often discussed (e.g., Elmegreen in “Evolution of the ISM”, ASP 1990)

- Collisional agglomeration of smaller clouds
- Formation from HI, e.g. by “gravo-thermal” instability
- Shocks in a turbulent ISM, generated by outflows from SN remnants

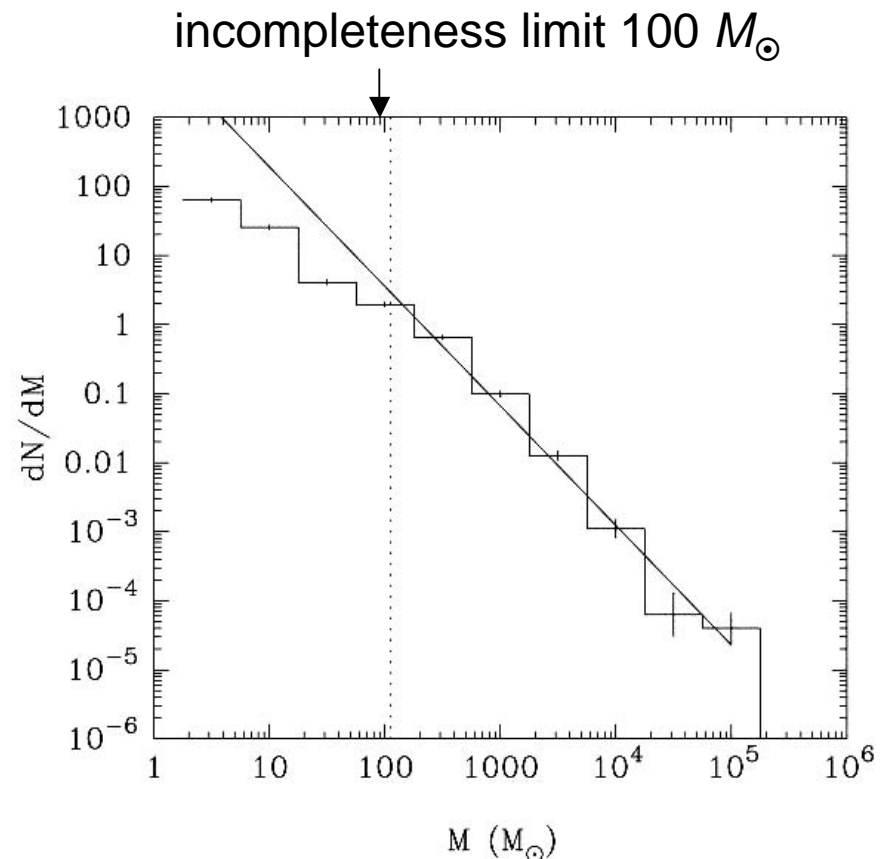
If GMCs are formed from the coalescence (agglomeration) of molecular fragments, where is that gas? Is it the chaff seen in spiral arms and in the vicinity of GMCs? But if star formation has already taken place, would the precursor gas still be observable?

# Agglomeration

Heyer & Terebey (ApJ 502 265 1998) catalog ~ 1600 clouds in the FCRAO survey and find  $dN/dM \sim M^{-1.75}$ .

The single power law says that the non-GMC “chaff” ( $M < 10^3 M_\odot$ ) appears to belong to the same parent population. Does it have the same origin as self gravitating clouds?

Blitz & Williams argue that the timescales for formation and destructions times are the same order of magnitude (tens of Myr). So in steady state, the mass in low-density molecular clouds and GMCs should be ~ the same. This *not* being the case, they conclude that GMCs form from HI.





## 4. Structure of Molecular Clouds

CO maps show that molecular gas is heterogeneous.

*What is the topology of molecular clouds?*

*Is it useful to talk about discrete structure?*

Blitz & Williams discuss three levels of structure: **clouds**, **clumps**, and **cores**, illustrated by the following maps of the Rosette Molecular Cloud in CO, C<sup>18</sup>O, and CS:

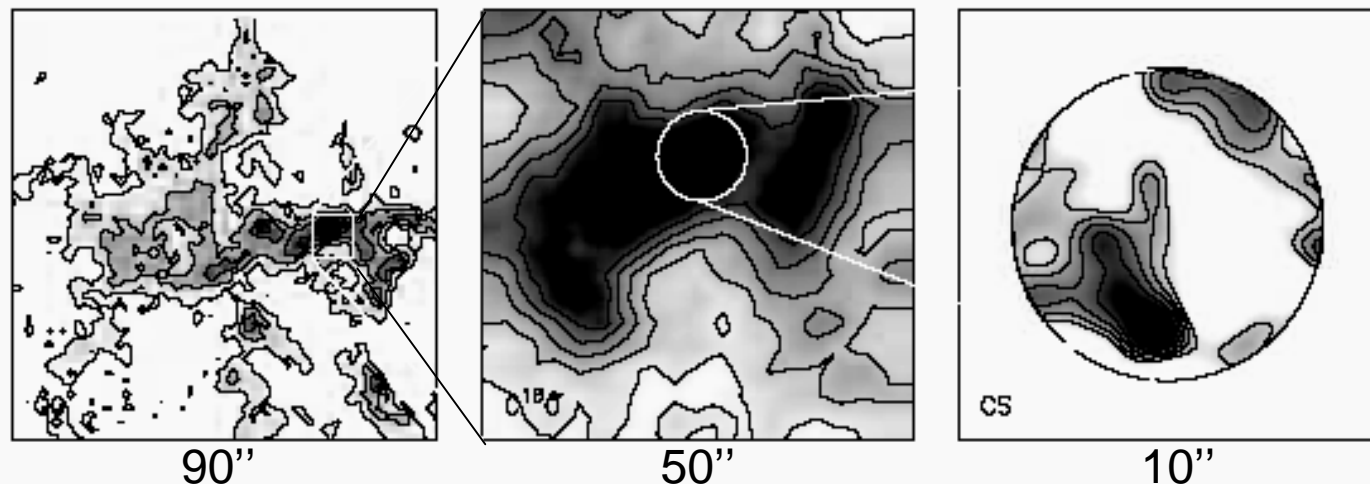


*Figure 4.* Hierarchical cloud structure. The three panels show a representative view from cloud to clump to core. The bulk of the molecular gas (cloud; left panel) is best seen in CO which, although optically thick, faithfully outlines the location of the H<sub>2</sub>. Internal structure (clumps; middle panel) is observed at higher resolution in an optically thin line such as C<sup>18</sup>O. With a higher density tracer such as CS, cores (right panel) stand out. The observations here are of the Rosette molecular cloud and are respectively, Bell Labs (90''), FCRAO data (50''), and BIMA data (10'').

# Clumps in GMCs

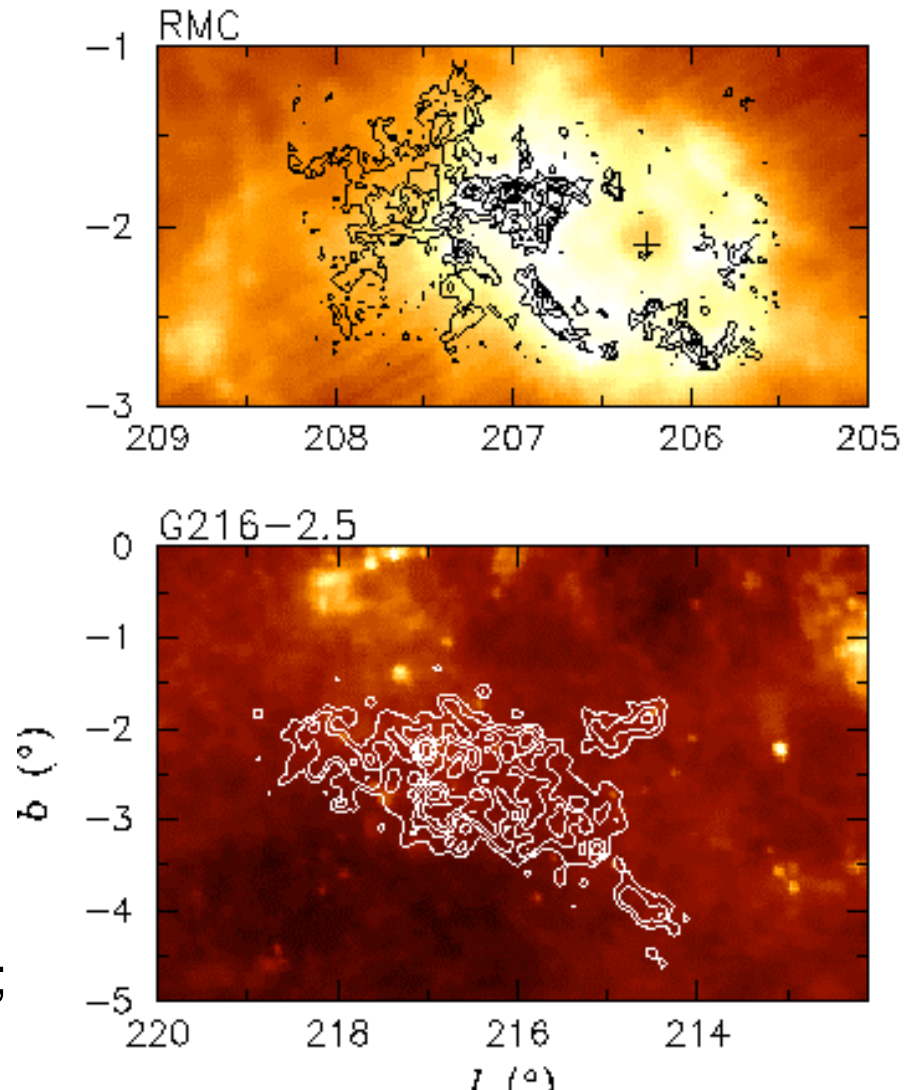
Williams et al (ApJ 428 693 1994)  
analyzed the  $\sim 100$   $^{13}\text{CO}$  1-0  
clumps in both the Rosette and the  
Maddalena Molecular Clouds

Both clouds have similar masses  
 $\sim 10^5 M_{\odot}$ , but orders of magnitude  
different star formation rates, as  
traced by FIR dust emission:

- Rosette:  $\sim 17$  OB plus numerous  
embedded sources
- G216-2.5: no OB stars and  
low  $L_{\text{IR}} / M(\text{H}_2) < 0.07 L_{\odot}/M_{\odot}$
- Star formation in the RMC occurs  
in its gravitationally bound clumps;  
the MMC has none.

**Why is there no star formation in the  
Maddalena cloud?**

ay216

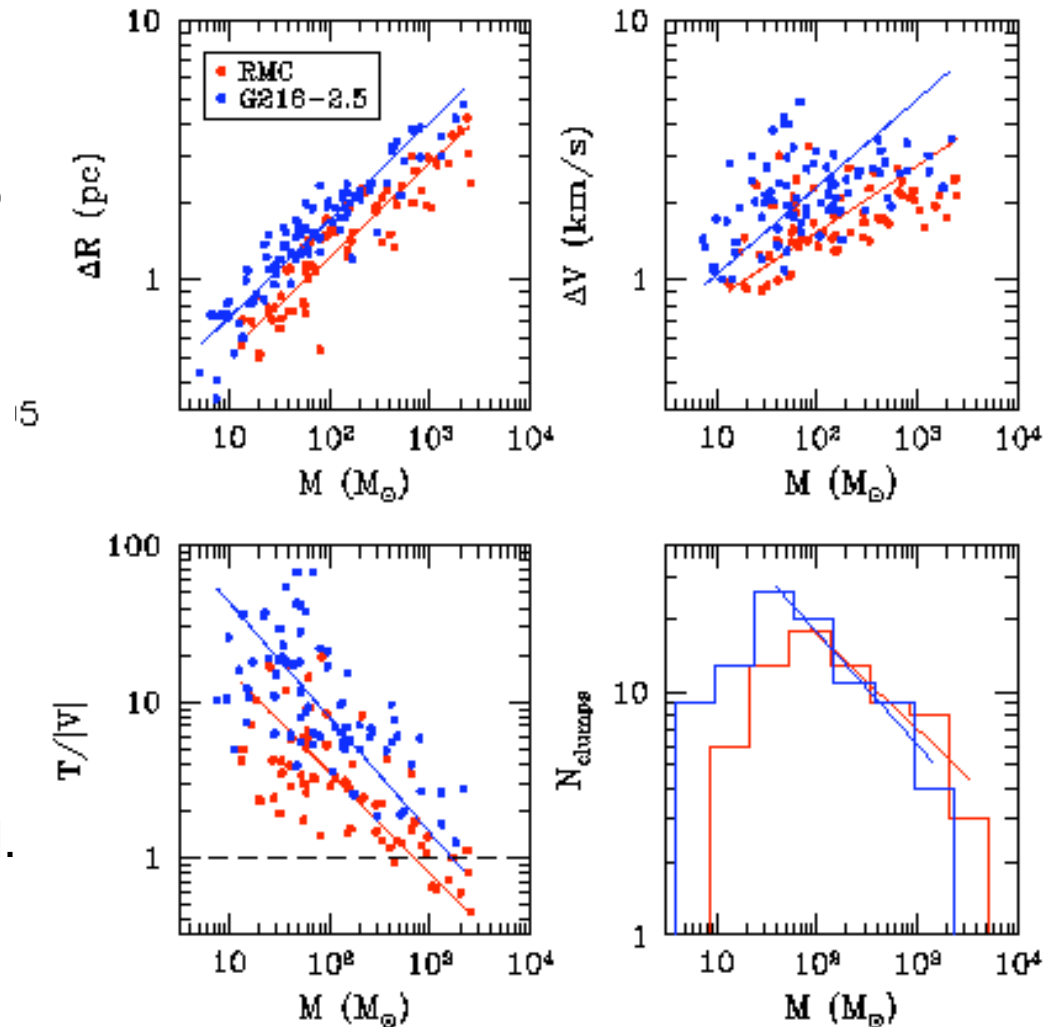


CO luminosity contours overlaid  
On IRAS 100  $\mu\text{m}$  intensity

# Clump Properties

Williams et al (ApJ 428 693 1994)

- Clump masses derived with an X-factor calibrated with  $^{13}\text{CO}$   $\sim 1/2$  of the galactic average
- Spatial resolution for both clouds is similar  $\sim 0.7$  pc.
- Clumps are more or less similar; those in G216-2.5 are bigger for a given mass and have larger line widths.
- Although both clouds are bound, none of the clumps in G216-2.5 are individually bound.



## 5. Molecular Cloud Cores

- Star formation occurs in the densest parts of GMCs known as molecular cloud cores.
- About 1/2 of known cores are luminous IR sources powered by stars in the process of newborn stars.
- Molecular core properties provide the initial conditions for star formation and may determine the properties of the stars they form.
- Keys to observing cores are molecular lines that trace high density rather than low density gas and IR measurements of warm dust heated by newborn stars.

### References

Bergin & Tafalla, ARAA 45 339 2007  
Benson & Myers, ApJS 71 743 1989  
Jijina et al. ApJS 125 161 1999

## Dense Gas Tracers

Molecule	Transition	Frequency (GHz)	$E/k$ (K)	$n_{\text{crit}}$ (cm <sup>-3</sup> ) @ 10 K	$n_{\text{eff}}$ (cm <sup>-3</sup> ) @ 10 K
CS	1-0	49.0	2.4	$4.6 \times 10^4$	$7.0 \times 10^3$
	2-1	98.0	7.1	$3.0 \times 10^5$	$1.8 \times 10^4$
	3-2	147.0	14	$1.3 \times 10^6$	$7.0 \times 10^4$
HCO <sup>+</sup>	1-0	89.2	4.3	$1.7 \times 10^5$	$2.4 \times 10^3$
	3-2	267.6	26	$4.2 \times 10^6$	$6.3 \times 10^4$
HCN	1-0	88.6	4.3	$2.6 \times 10^6$	$2.9 \times 10^4$
	3-2	265.9	26	$7.8 \times 10^7$	$7.0 \times 10^5$
H <sub>2</sub> CO	$2_{12}-1_{11}$	140.8	6.8	$1.1 \times 10^6$	$6.0 \times 10^4$
	$3_{13}-2_{12}$	211.2	17	$5.6 \times 10^6$	$3.2 \times 10^5$
	$4_{14}-3_{13}$	281.5	30	$9.7 \times 10^6$	$2.2 \times 10^6$
NH <sub>3</sub>	(1,1)	23.7	1.1	$1.8 \times 10^3$	$1.2 \times 10^3$
	(2,2)	23.7	42	$2.1 \times 10^3$	$3.6 \times 10^4$

See Schoier et al. A&A 432 369 2005 for dipole moments etc.



# Measurement of Core Temperatures

Although almost any optically-thick rotational ladder may work, the ***inversion spectrum*** of  $\text{NH}_3$  is the most useful. The basic reference is Townes & Schawlow, Ch. 12.

In the ground state, the N atom is located on either side of the 3 H atoms in the plane. To get to the other side, it has to tunnel through the potential barrier, whose height is  $\sim 2,000 \text{ cm}^{-1}$ . The tunneling frequency is very small and is in the cm radio band.

Similar splittings occur for methanol ( $\text{CH}_3\text{OH}$ ).

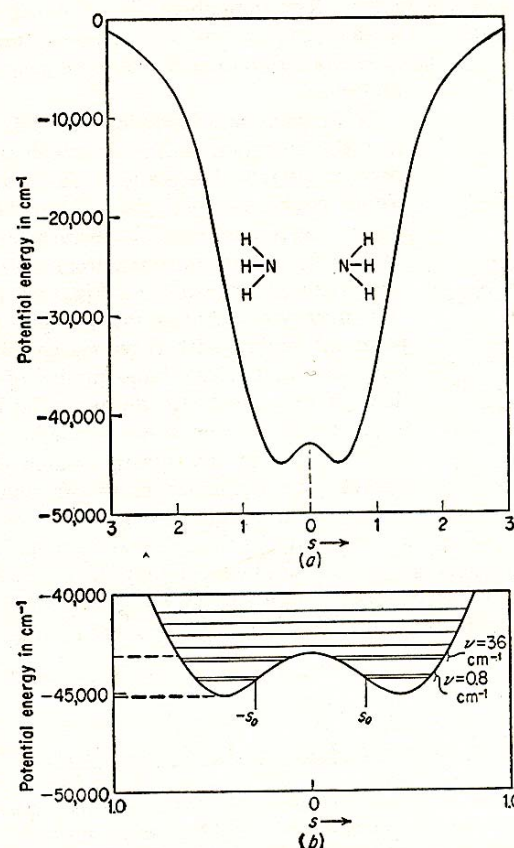


FIG. 12-1. Potential curve of  $\text{NH}_3$ . The variable  $s$  is a measure of the distance between the nitrogen and the plane of the hydrogens. (b) shows the lower part of the potential curve in more detail, and the energy levels.

# NH<sub>3</sub> Temperature Measurement

NH<sub>3</sub> is a symmetric rotor with a dipole moment of 1.48 D. The allowed *rotational* transitions satisfy  $|\Delta J| = 1$  and  $\Delta K = 0$ , but the frequencies are so high they require space observations.

But the levels are split by tunneling in the 25-GHz band that depends on (J,K). The transitions usually observed are at the bottom of each K-ladder. The splittings of these (K,K) levels are:

(1,1)	23.694 GHz
(2,2)	23.723
(3,3)	23.870
(4,4)	24.139
(5,5)	24.533
(6,6)	25.056

ay216

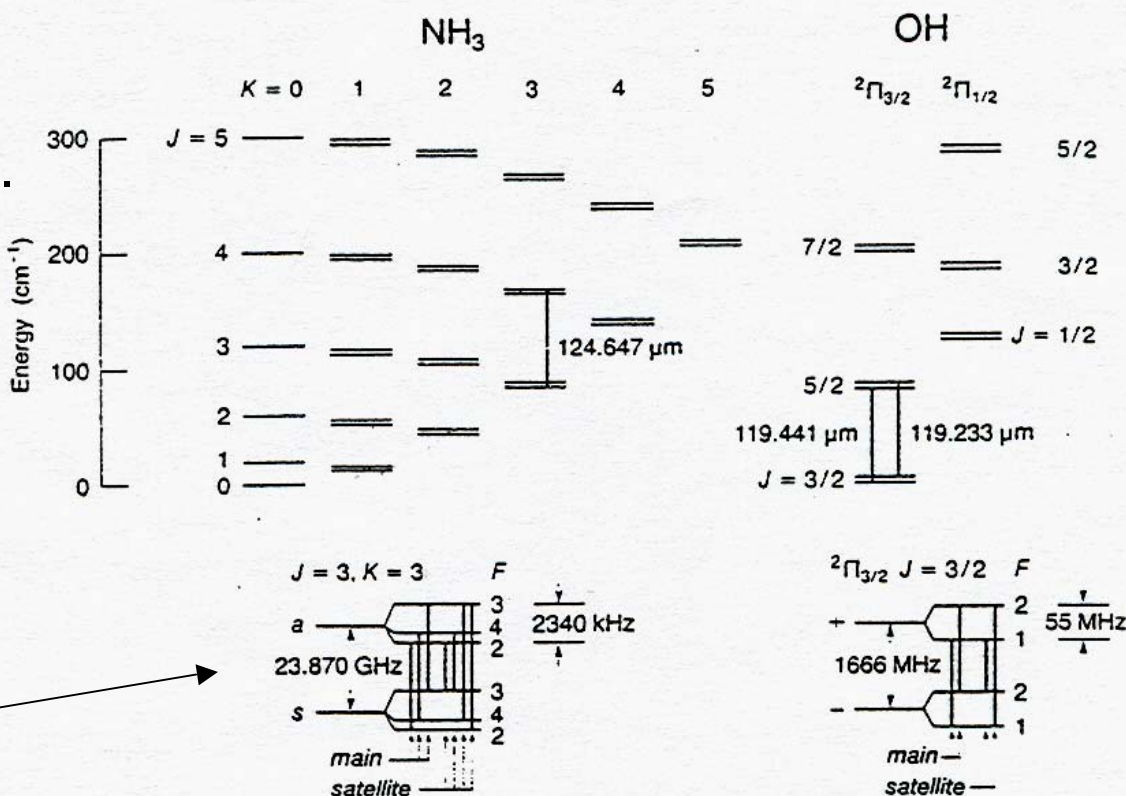


Fig. 5. Rotational levels of NH<sub>3</sub> (left) and OH (right) (adapted from Watson 1982)

The hyperfine splittings are also shown.

# NH<sub>3</sub> Temperatures

The beauty of measuring the inversion transitions of the NH<sub>3</sub> ( $K,K$ ) levels is that they span a large range of excitation temperature but require measurements in just one radio band (using the same instrumentation for all transitions). The transitions listed above cover the temperature range up to 500 K.

This is to be contrasted with a non-hydride rotor like CO where a large range of excitation temperatures can only be achieved by using different telescopes with different resolution.

The often used ( $J,K$ )=(1,1) level occurs at 1.27 cm and has a fairly high critical density.

# Shapes of Molecular Cloud Cores

Lada et al. 376 561 1991

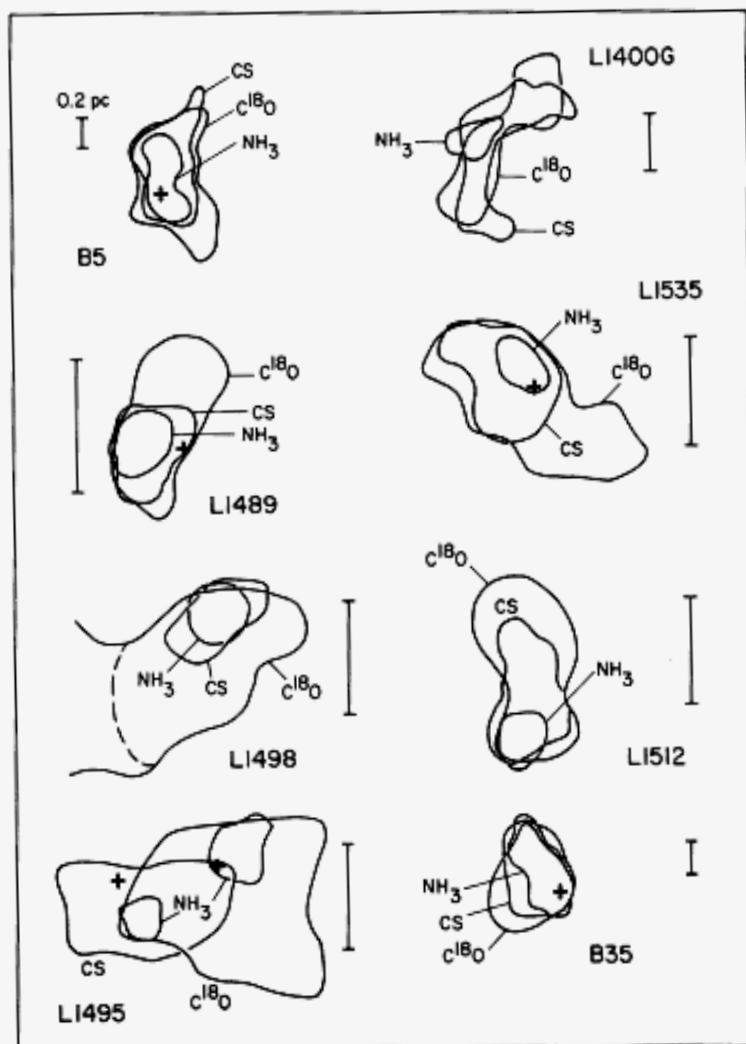


FIG. 1a

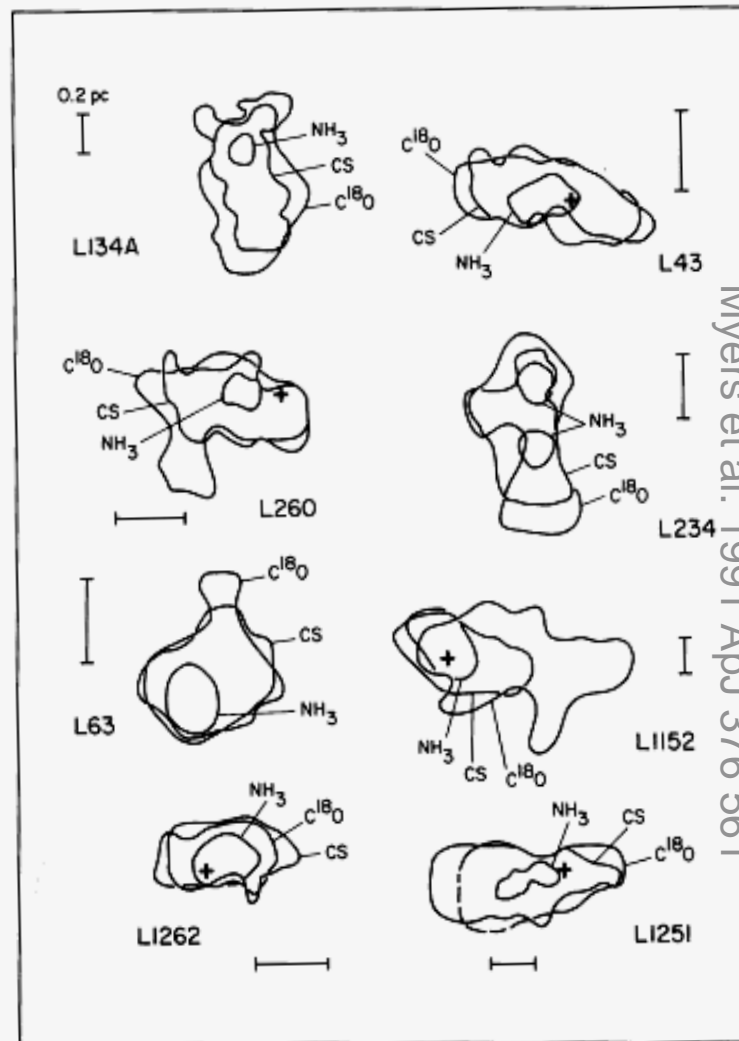


FIG. 1b

FIG. 1.—Half-maximum intensity contours of 16 dense cores in dark clouds, in the 1.3 cm  $(J, K) = (1, 1)$  lines of  $\text{NH}_3$ , from Benson & Myers (1989), and in the 3.0 mm  $J = 2 \rightarrow 1$  line of CS, and the 2.7 mm  $J = 1 \rightarrow 0$  line of  $\text{C}^{18}\text{O}$ , from Fuller (1989). For each map, North is up, East is left, and the linear scale 0.2 pc is indicated. A cross indicates an associated star.

Notice the different map sizes for CO, CS &  $\text{NH}_3$

ayz 10

# Survey of 264 NH<sub>3</sub> Cores

Jijina et al. (ApJS 126 161 1999)

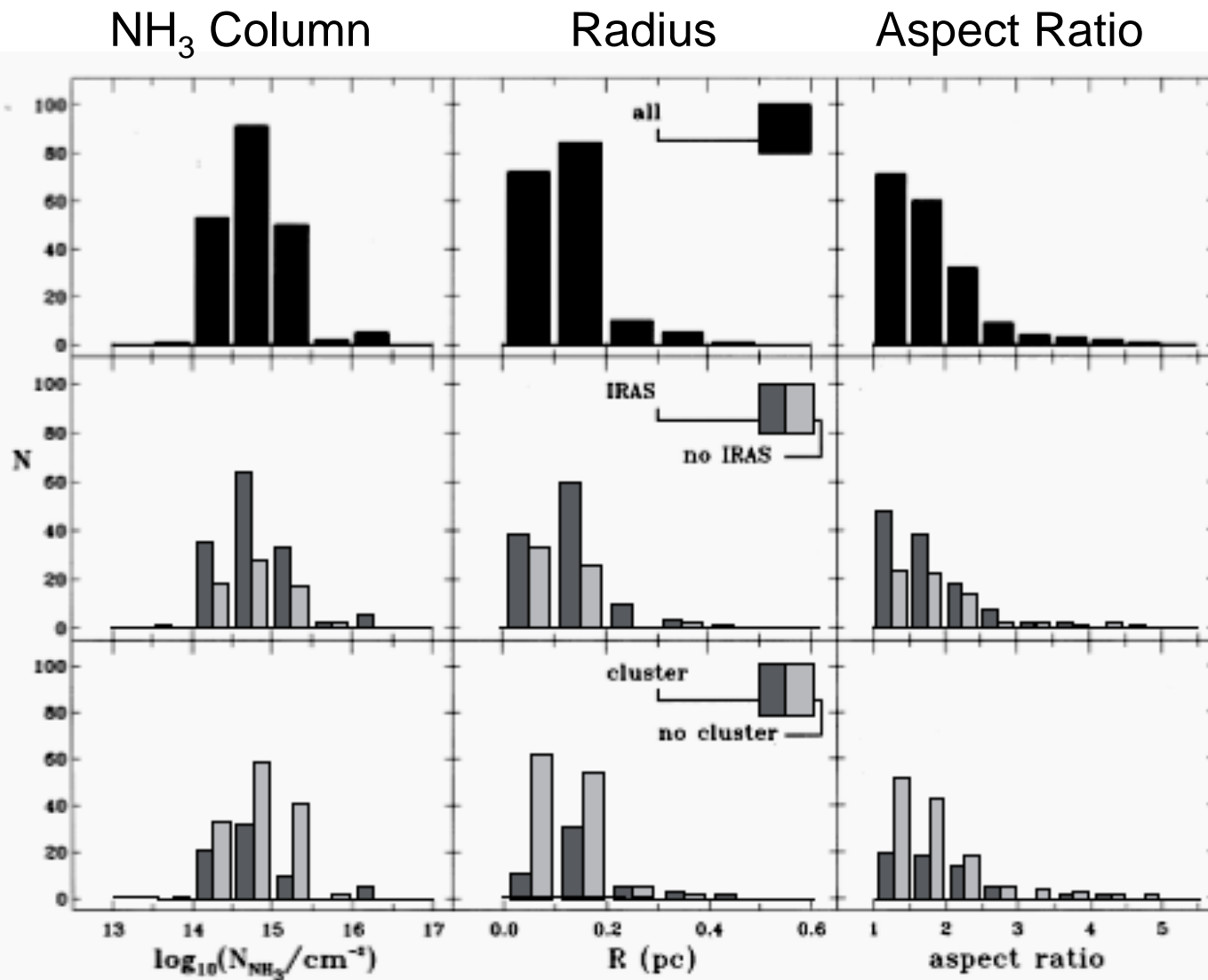


FIG. 1.—Distributions of the core gas properties; column densities,  $N_{\text{NH}_3}$  ( $\text{cm}^{-2}$ ), core sizes,  $R$  (pc), and aspect ratios,  $a/b$ , for the sum total sample containing all cores as well as for subsamples defined by the *IRAS* and cluster criteria. Refer to Tables B1–B3 for the statistics and to § 3 for a discussion.



# Jijina et al. $\text{NH}_3$ Core Survey

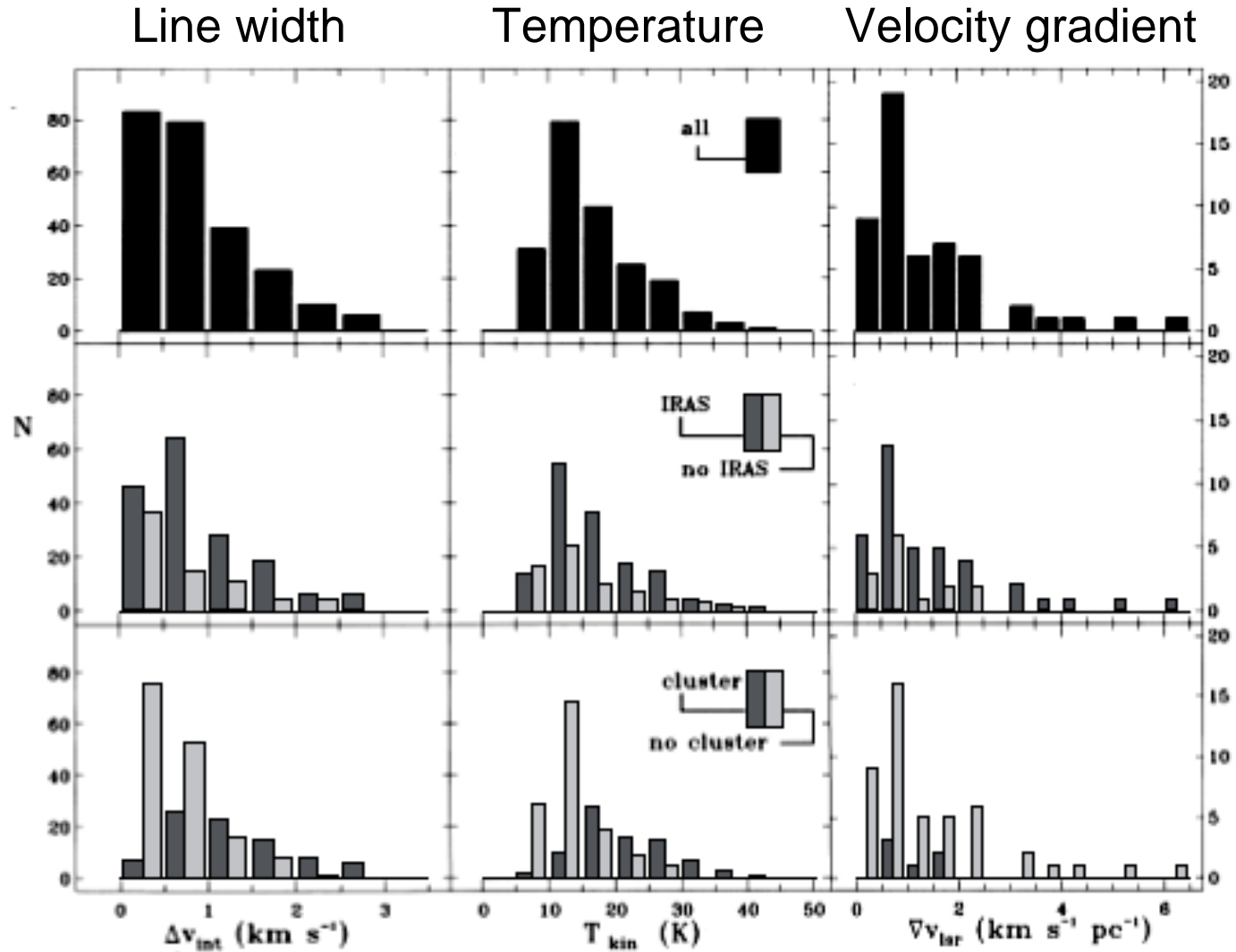
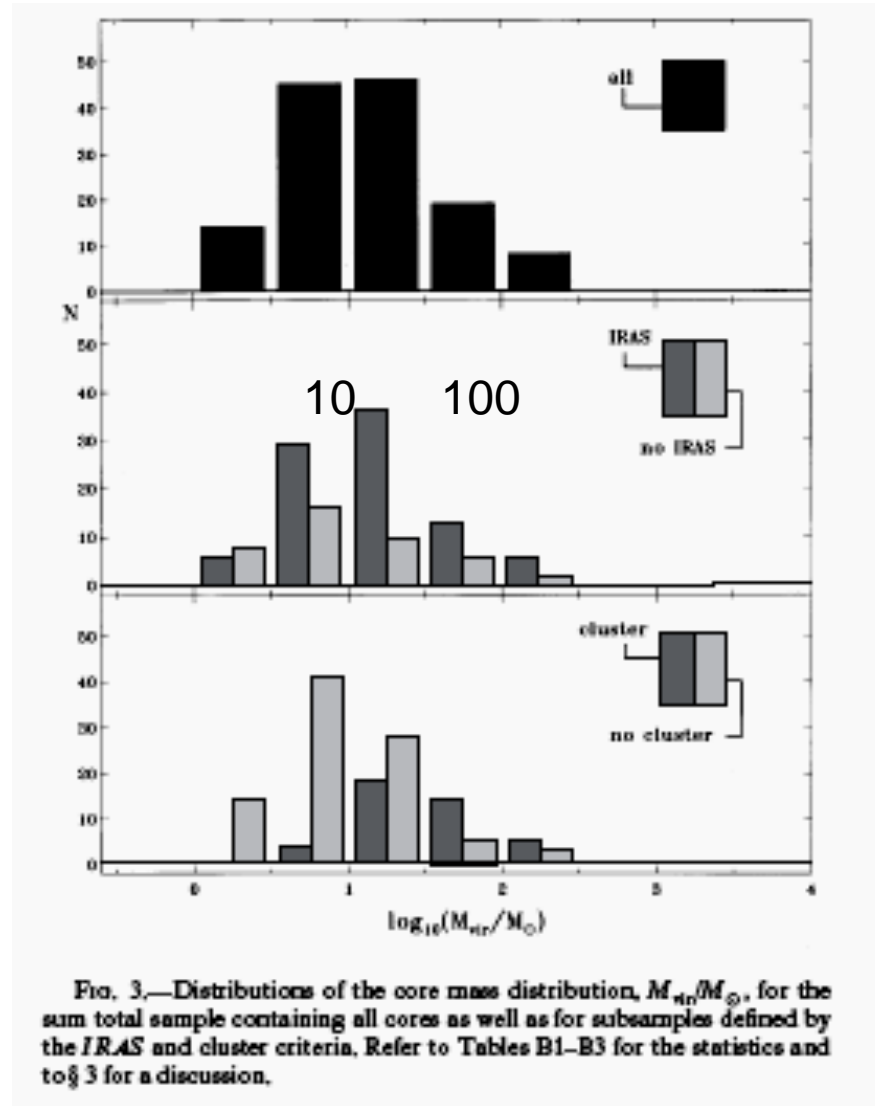


FIG. 2.—Distributions of the core gas properties: intrinsic velocities,  $\Delta v_{\text{int}}$  ( $\text{km s}^{-1}$ ), kinetic temperatures,  $T_{\text{kin}}$  (K), and velocity gradients,  $\nabla v_{\text{lsr}}$  ( $\text{km s}^{-1} \text{ pc}^{-1}$ ), for the sum total sample containing all cores as well as for subsamples defined by the *IRAS* and cluster criteria. Refer to Tables B1–B3 for the statistics and to § 3 for a discussion.

# Jijina et al. $\text{NH}_3$ Core Survey

## Mass distribution



# Observed Core Properties

1. associated with star formation, e.g., 50% or more have embedded protostars ( SPITZER has found a few more)
2. elongated (aspect ratio  $\sim 2:1$ )
3. internal dynamics may be dominated by thermal or turbulent motion,

$$\Delta v_{\text{FWHM}}^2 = \Delta_{\text{turb}}^2 + 8 \ln 2 \left( \frac{kT}{m} \right)$$

e.g., equally split for  $\text{NH}_3$  cores. Note that

$$\Delta v_{\text{th}} = \sqrt{8 \ln 2 \left( \frac{kT}{m} \right)} = 0.675 \text{ km s}^{-1} \sqrt{\frac{m_{\text{H}}}{m} \left( \frac{10\text{K}}{T} \right)}$$

is typically  $\sim 0.1 - 0.2 \text{ km s}^{-1}$

# Non-thermal vs. Thermal Line Widths

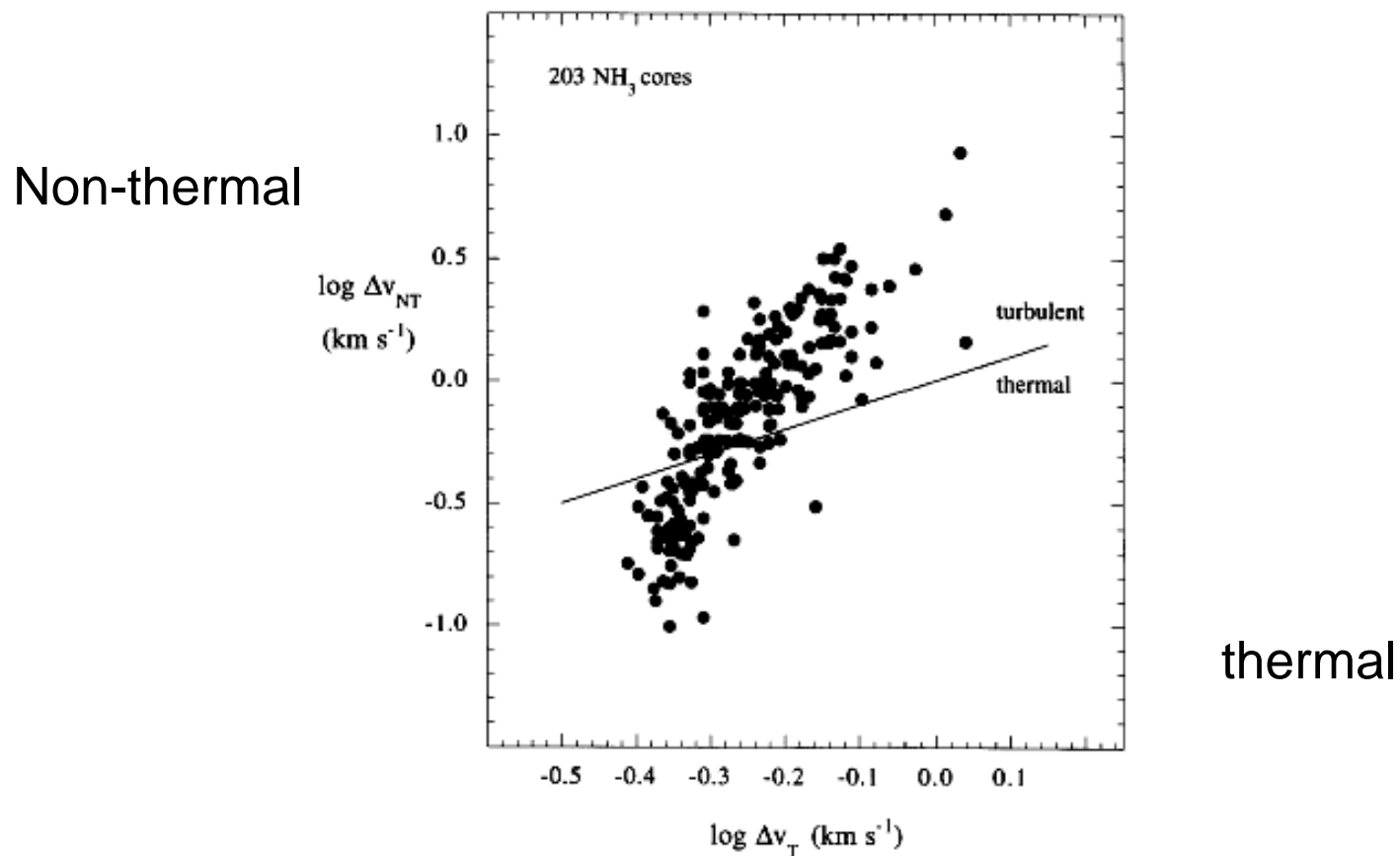


*Figure 6.* Nonthermal and thermal line widths in NH<sub>3</sub> dense cores. The FWHM of the distribution of nonthermal motions,  $\Delta v_{NT}$ , increases rapidly with the corresponding FWHM of the distribution of thermal motions of the molecule of mean mass,  $\Delta v_T$ . Thus turbulent cores tend to be warm, and quiescent cores tend to be cool (JMA).

Jijina et al. ApJS 126 161 1999

# Observed Core Properties

4. temperature:  $T \sim 10 - 20$  K

5. size:  $R \sim 0.1$  pc

6. ionization:  $x_e \sim 10^{-7}$

7. size-linewidth relation  
 $R \sim \sigma^p$ ,  $p = 0.3-0.7$

8. approximate virial  
equilibrium

9. mass spectrum: similar to  
GMCs.

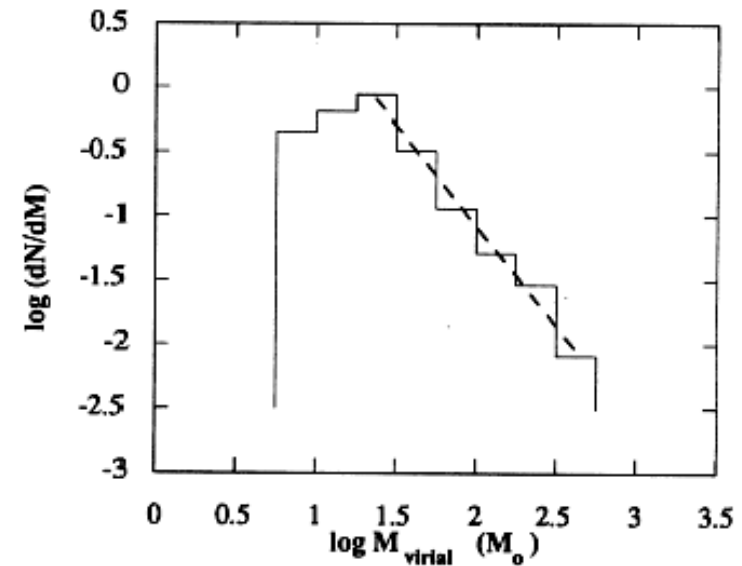


Figure 6. The mass spectrum of dense cores in the L 1630 cloud from the study of LBS. The spectrum can be characterized by a power law with an index of -1.6.

face that different definitions of clumps were employed in each case [26, 122].